Attenuation of Earthquake Ground Motion in Japan Including Deep Focus Events

by Gilbert L. Molas and Fumio Yamazaki

Abstract New attenuation equations for peak ground acceleration and velocity for Japan are developed. The equations are derived using extensive data recorded by the new JMA-87–type accelerometers, which do not require instrumental corrections that the older SMAC-type accelerometers do. Earthquakes with depths up to 200 km are used to make the equation applicable to subduction zone regions, which are common in Japan. Effects of depth and local site on the attenuation are considered simultaneously with the distance dependence and magnitude dependence using a two-stage regression procedure to separate the magnitude dependence from the distance dependence. Since the resulting normal equations become singular, an iterative partial regression algorithm is proposed. It is found that for the same magnitude and distance, peak ground motion increases as depth increases. The variation of the station coefficients with respect to the corresponding soil-type classification is quite wide. The station coefficients for the peak ground acceleration are found to be weakly correlated with the general soil classification, while a stronger correlation was found for the peak ground velocity. The resulting attenuation relations are given by

$$\log_{10} \text{PGA} = 0.206 + 0.477 M_J - \log_{10} r - 0.00144r + 0.00311h + c_i^a,$$
$$\log_{10} \text{PGV} = -1.769 + 0.628 M_J - \log_{10} r - 0.00130r + 0.00222h + c_i^v,$$

where PGA (cm/sec^2) and PGV (cm/sec) are the larger of the peak accelerations and velocities from two horizontal components, M_J is the JMA magnitude, r is the closest distance to the fault rupture, h is the depth, and c_i is the station coefficient of the recording station. The mean of the coefficients of the JMA stations is given by $c_i = 0$.

Introduction

As more ground motion records are obtained, it is possible to improve our understanding of attenuation characteristics of strong ground motion. Many attenuation relationships of strong ground motion that have been developed only consider "shallow" earthquakes (i.e., with focal depth less than about 30 to 60 km). Seismic hazard analyses for many subduction zone regions, however, require attenuation laws that consider focal depths much larger than for shallow faulting. The Kushiro-Oki earthquake on 15 January 1993 (M_{JMA} = 7.8, focal depth = 103.2 km) has demonstrated the importance of earthquakes with focal depths of about 100 km or more. Crouse et al. (1988) and Annaka and Nozawa (1988) provide the few studies regarding subduction zone earthquakes, which usually have larger focal depths. In Japan, where most events are from subduction zones, attenuation relationships commonly use data with focal depths of up to 60 km. The attenuation relation of Annaka and Nozawa (1988) is one of the few that use data with focal depths of up to 100 km.

Many attenuation relationships developed for Japan are based on strong ground motion recorded by SMAC-B2 accelerometers. Since these accelerometers suppress high frequencies, their use in attenuation studies necessitates correction procedures (Kawashima et al., 1982, 1986). Recently, Fukushima and Tanaka (1990) developed an attenuation relationship for Japan, but the data used for the analysis included old uncorrected SMAC-B2 records.

In 1987, the Japan Meteorological Agency (JMA) started to deploy the new JMA-87–type accelerometers in recording stations throughout Japan. The new accelerometers have a flat sensitivity from 0.05 to 10 Hz and can measure accelerations from 30 × 10^{-3} to 980 cm/sec^2 for periods from 1 sec to 10 min (JMA, 1991). Data supplied by JMA from these accelerometers do not need correction; thereby avoiding errors involved in the correction procedure.

This study uses data recorded by these new accelerometers at the JMA stations (Fig. 1). The accelerometers are placed on small foundations that are detached from the struc-

(a)

(b)
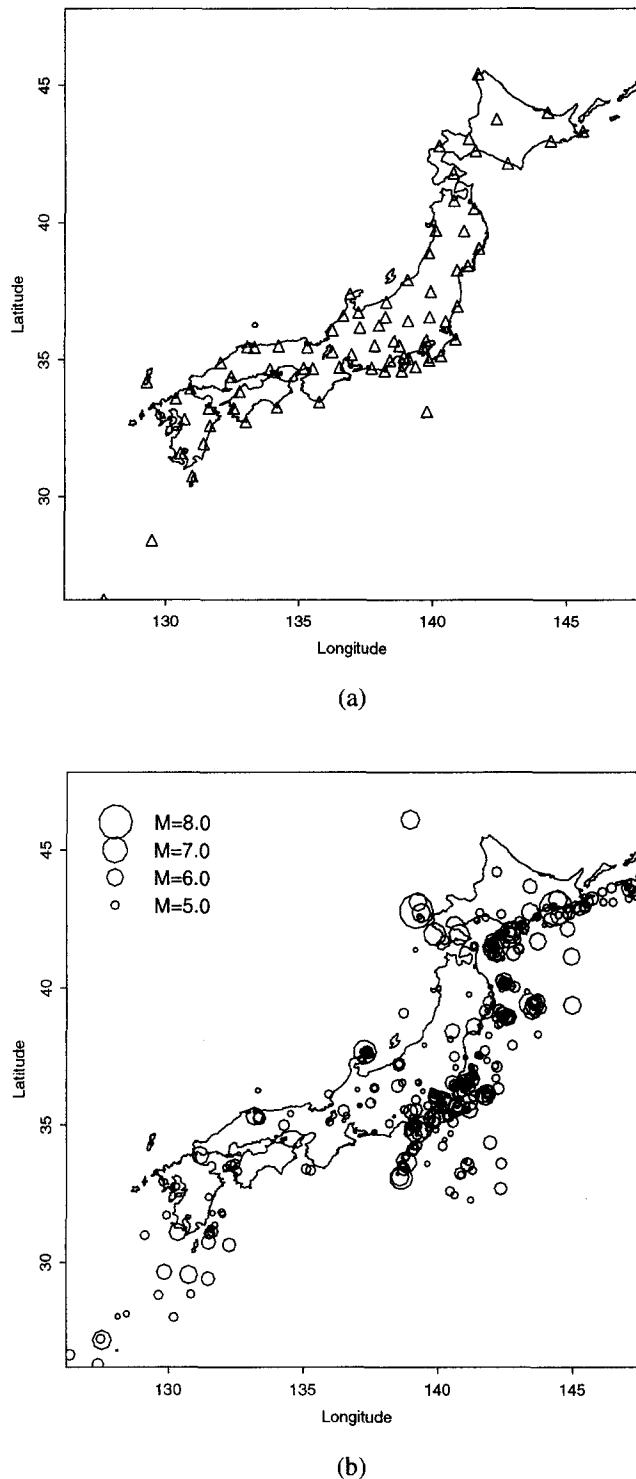
Figure 1. Location of (a) JMA recording stations (triangles) and (b) epicenters of earthquakes (circles) used in this study (size of the circle denotes magnitude).

ture that houses the accelerometers, so that the records may be considered as free field. The data include records from earthquakes with focal depths greater than 100 km. This presents a unique opportunity to study the attenuation characteristics of earthquakes with large focal depths. Since the recording stations are fixed and each station has several records, we can also study the effect of local site on the attenuation of earthquake ground motions.

Data

We use the recorded acceleration time histories for the period from 1 August 1988 to 31 December 1993. The data set includes records from recent damaging earthquakes like the 15 January 1993 Kushiro-Oki earthquake, 7 February 1993 Noto Peninsula-Oki earthquake (M_{JMA} = 6.6, focal depth = 24.8 km), and the 12 July 1993 Hokkaido Nansei-Oki earthquake (M_{JMA} = 7.8, focal depth = 34 km). Figure 1 shows the locations of the JMA stations and the epicenters of earthquakes used in this study. Records with peak ground accelerations (PGA) less than 1.0 cm/sec² in one horizontal component are omitted. Examination of the records revealed that weaker records are not reliable due to the resolution (± 0.03 cm/sec²) of the recording instrument. Events whose focal depths are zero are also excluded from the analysis. The resulting data set includes only a few data earthquakes with focal depth greater than 200 km. Therefore, due to the lack of sufficient data, records from events whose focal depths are greater than 200 km are excluded.

The final data set consists of 2166 pairs of orthogonal horizontal components from 387 events recorded at 76 JMA stations. To get velocity time histories, the acceleration time histories are integrated in the frequency domain after applying a low-cut filter with a cosine-shaped transition from 0.01 to 0.05 Hz to remove long-period noise.

Figure 2 shows the distribution of the JMA magnitude, depth, distance, and PGA of the data used in this study and the histogram of the number of records per station. The distribution of magnitude-distance shows a positive correlation between magnitude and distance. This is a common observation on Japanese data distribution (Fukushima and Tanaka, 1990) and is caused by the fact that seismic waves produced by large-magnitude earthquakes tend to propagate farther than those produced by small-magnitude earthquakes.

Attenuation Model

There are many models used in attenuation studies. Attenuation studies are reviewed by Boore and Joyner (1982), Joyner and Boore (1988), and Campbell (1985). In this study, the initial model is based on the attenuation of body waves in an elastic medium from a point source (e.g., Joyner and Boore, 1981; Abrahamson and Litehiser, 1989; Ohno et al., 1993) and given as

(a)

(b)

(c)

(d)
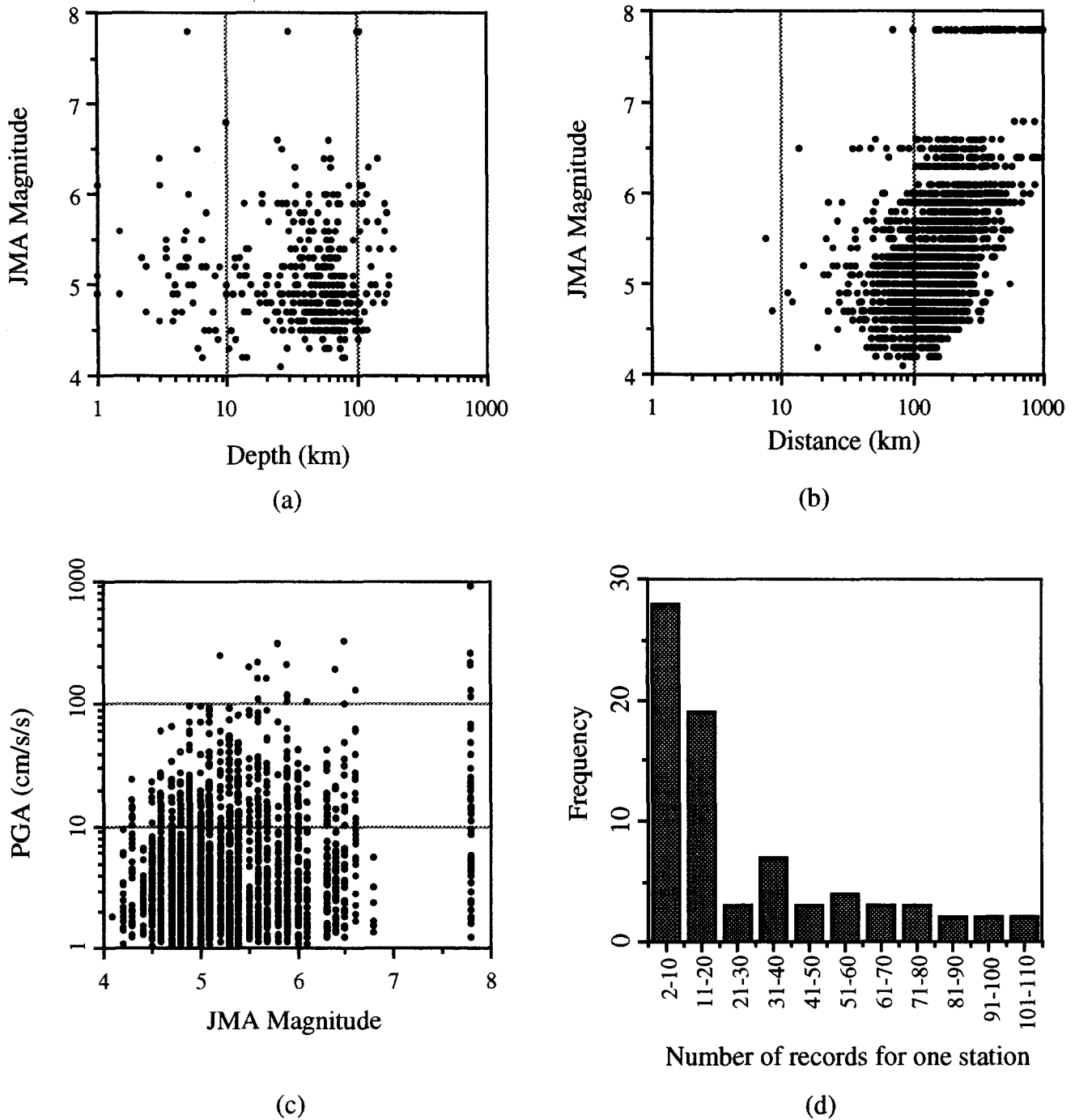
Figure 2.   Distribution of (a) depth, (b) distance, and (c) magnitude and peak ground acceleration of the records used in this study and (d) the histogram of the number of records per station.

$$\log y = b_0 + b_1 M + b_2 r + b_3 \log r, \qquad (1)$$

where y is the ground motion index under consideration. In this study, y is taken as the larger maximum amplitude of the two horizontal components, M is the JMA magnitude, r is the slant distance between the source and the recording station, and the b_is are the coefficients to be determined. It must be noted that the definition of the JMA magnitude is

different for focal depths greater than 60 km. The definition for deep events considers the effect of depth and attenuation so that the magnitude can be used continuously from shallow to deep events. The term $b_2 r$ represents anelastic attenuation, and the term $b_3 \log r$ represents geometric spreading. Strictly speaking, b_3 should be -1.0, but we unconstrain b_3 to allow for approximations in the model. The location of the source is generally assumed to be the center of energy release,

which could be estimated by the size of the ruptured fault or by the centroid of the aftershock cluster, if aftershocks are recorded. In the near field, the definition of distance becomes critical (Boore and Joyner, 1982), especially for earthquakes with a large fault extent. If the distance is redefined with respect to the fault extent, the attenuation in the near field becomes consistent with the attenuation of the far field (Singh et al., 1989; Ohno et al., 1993). In this study, we define r as the shortest distance from the recording site to the fault extent. However, published reports of fault extent and orientation are difficult to find or are nonexistent for the events in the data set, except for two large earthquakes of magnitude 7.8, namely, the 1993 Kushiro-Oki earthquake (Kagami, 1993) and the 1993 Hokkaido-Nansei-Oki earthquake (Nakanishi and Kikuchi, 1993). Most of the records are in the far field, and the third largest event with records close to the fault has a magnitude of 6.6. For the other records, we use the hypocentral distance. Since the effect on the regression of the change in distance definition is small in the far field and for small events, the use of hypocentral distances is practical and justified.

Ground motion of deeper earthquakes is generally stronger than that of shallow earthquakes with the same magnitude and source distance. Figure 3 shows the recorded PGAs for the Kushiro-Oki and the Hokkaido-Nansei-Oki earthquakes, both with a JMA magnitude of 7.8. The former has a focal depth of 103.2 km, while the latter has a focal depth of 34 km. It can be seen clearly that the ground motion for the Kushiro-Oki earthquake is significantly stronger for the same distance even though they have the same magnitude. An additional regressor variable for the depth to account for this effect can improve the regression fitting (Crouse et al., 1988; Annaka and Nozawa, 1988).

The effect of local ground condition is another important factor. Attenuation equations are commonly defined separately for rock and soil sites. Some use three or four soil-type classifications. A common technique to consider the ground condition is to use a dummy variable for each ground type (McGuire, 1978; Kawashima et al., 1986). Since the recording stations in this case are fixed and many records come from a given site, it is possible to resolve the local site effect for each station. This effect can be verified by examining the residuals with respect to the recording station. The regression is then performed by assigning a dummy variable for each site (Draper and Smith, 1981). The regression model is then given by

$$\log y = b_0 + b_1 M + b_2 r + b_3 \log r + b_4 h + c, \quad (2)$$

where h is the depth in kilometers of the point in the fault plane that is closest to the recording site and c is a coefficient representing the local site effect at the recording site.

A preliminary analysis is performed to verify the significance of the depth term and station coefficient to the regression. Equations (1) and (2) are used to regress the 2166 data using least-squares fitting. The results of the preliminary
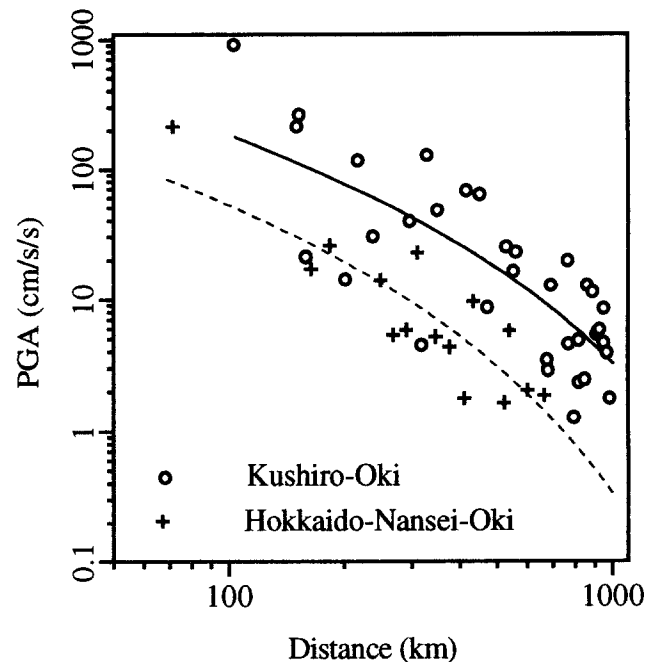
Figure 3.   Recorded peak ground acceleration for the 1993 Kushiro-Oki ($M_{\text{JMA}} = 7.8$, $M_w = 7.5$) and 1993 Hokkaido-Nansei-Oki ($M_{\text{JMA}} = 7.8$, $M_w = 7.7$) earthquakes with respect to the shortest distance to the fault. Lines show regression curves for the Kushiro-Oki (solid line) and the Hokkaido-Nansei-Oki (broken line) earthquakes using the relation log PGA $= b_0 + b_2 r - \log r$.

regressions are given in Table 1. Case 1, which is a least-squares solution of equation (1), gives an anelastic attenuation term that has an inadmissible sign (b_2 failed the t-test at the 95% confidence level) and a geometric spreading term that is not in accordance with theory (i.e., b_3 should be from 0 to -1.0). For case 2, the anelastic attenuation term is constrained to zero, but the geometric spreading term is still less than -1.0. For case 3, b_3 is constrained to -1.0 (spherical spreading), and b_2 is unconstrained. Here all the terms are within their physically admissible range. For case 3, we look at the behavior of the residuals to check for some trends.

Figure 4 shows the residuals with respect to the depth. We can see that there is a definite positive linear correlation between the residuals and the depth, especially in the range from 0 to 100 km. Case 4 in Table 1 gives the result when a depth term, $b_4 h$, is added to the regression equation. We can see a significant improvement in the R^2 statistic, which implies a better fit with the new model. The term R^2 or the square of the multiple correlational coefficient estimates the proportion of the variation in the response around the mean that can be attributed to terms in the model rather than random error.

Figure 2d shows the histogram of the number of records per station. Almost 40% of the stations have 21 or more data used in the analysis. This makes it useful to determine the

Table 1
Regression Constants for Preliminary Regression

Case	b_0	b_1	b_2	b_3	b_4	c_i^*	σ	R^2
1	1.5132	0.3604	0.00027	−1.3058	0.0	X	0.342	0.4209
2	1.2866	0.3695	0.0	−1.1994	0.0	X	0.342	0.4196
3	0.9540	0.3596	−0.00026	−1.0	0.0	X	0.344	0.3032
4	0.6879	0.3889	−0.00056	−1.0	0.00302	X	0.328	0.3667
5	0.3394	0.4486	−0.00089	−1.0	0.00259	O	0.279	0.5568

*O: c_is are calculated; X: c_is are constrained to zero.
Underlined values are constrained.
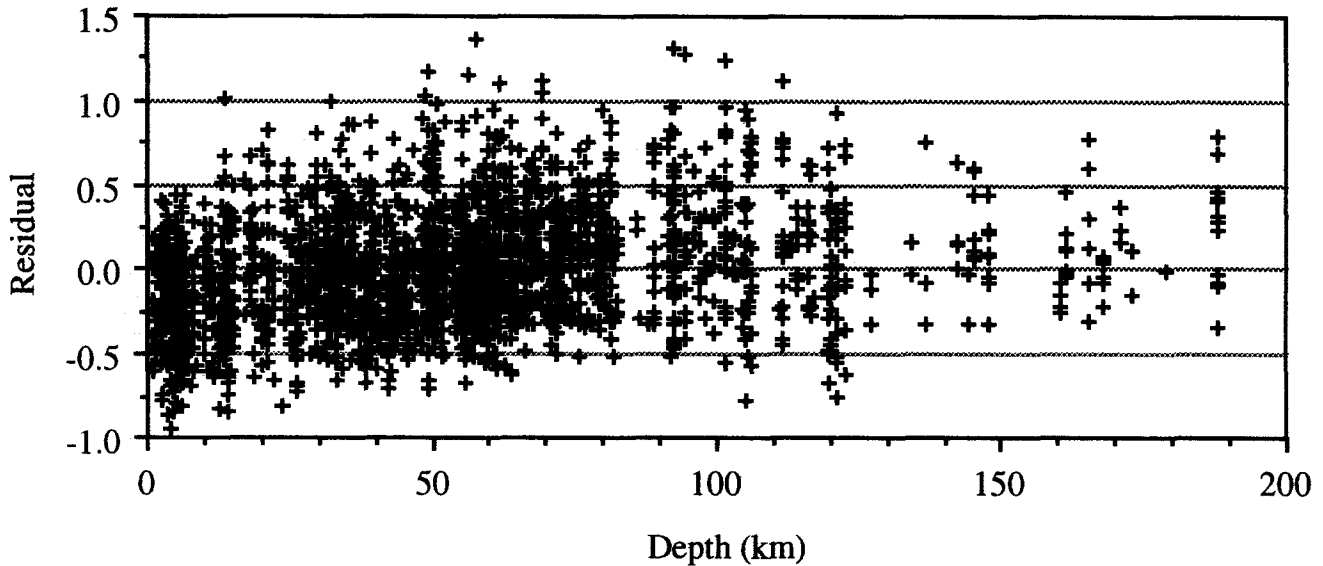
Figure 4. Residuals from the regression of log PGA with respect to the focal depth for case 3 of Table 1. A definite linear trend can be seen especially for depths of up to 100 km.

relative effects of the recording stations. Equation (2) can be expanded in matrix form as follows:

$$\begin{bmatrix} \log y_1 \\ \log y_2 \\ \vdots \\ \log y_n \end{bmatrix} = \begin{bmatrix} 1 & M_1 & r_1 & \log r_1 & h_1 & S_{1,1} & \cdots & S_{N-1,1} \\ 1 & M_2 & r_2 & \log r_2 & h_2 & S_{1,2} & \cdots & S_{N-1,2} \\ \vdots & \vdots & \vdots & \vdots & \vdots & \vdots & \vdots & \vdots \\ 1 & M_n & r_n & \log r_n & h_n & S_{1,n} & \cdots & S_{N-1,n} \end{bmatrix}$$

$$\begin{bmatrix} b_0 \\ \vdots \\ b_4 \\ c_1 \\ \vdots \\ c_{N-1} \end{bmatrix} + \begin{bmatrix} \varepsilon_1 \\ \varepsilon_2 \\ \vdots \\ \varepsilon_n \end{bmatrix}, \tag{3}$$

where n is the number of records, N is the number of recording stations, c_is are the station coefficients, and ε_j is the associated residual. The dummy variables, S_{ij}, are configured such that the mean of station coefficients is zero. For the jth

data recorded at station l, $S_{i\neq l,j} = 0$ and $S_{i=l,j} = 1$ except if the data is recorded at the last (Nth) station, then S_{ij} is taken as -1.0 for $i = 1$ to $N - 1$. In notation form,

$$Y = X\beta + \varepsilon, \tag{4}$$

and the least-squares solution is

$$b = (X^T X)^{-1} X^T Y, \tag{5}$$

where b is the estimator of β, and the expected value $E(b)$ is β.

The coefficient of the Nth station is

$$c_N = -\sum_{i=1}^{N-1} c_i. \tag{6}$$

Figure 5 shows the mean residuals and standard deviation (error bars) for each station for case 3. It can be seen that there is indeed a difference in the means of the residuals for each recording station. Case 5 on Table 1 shows the
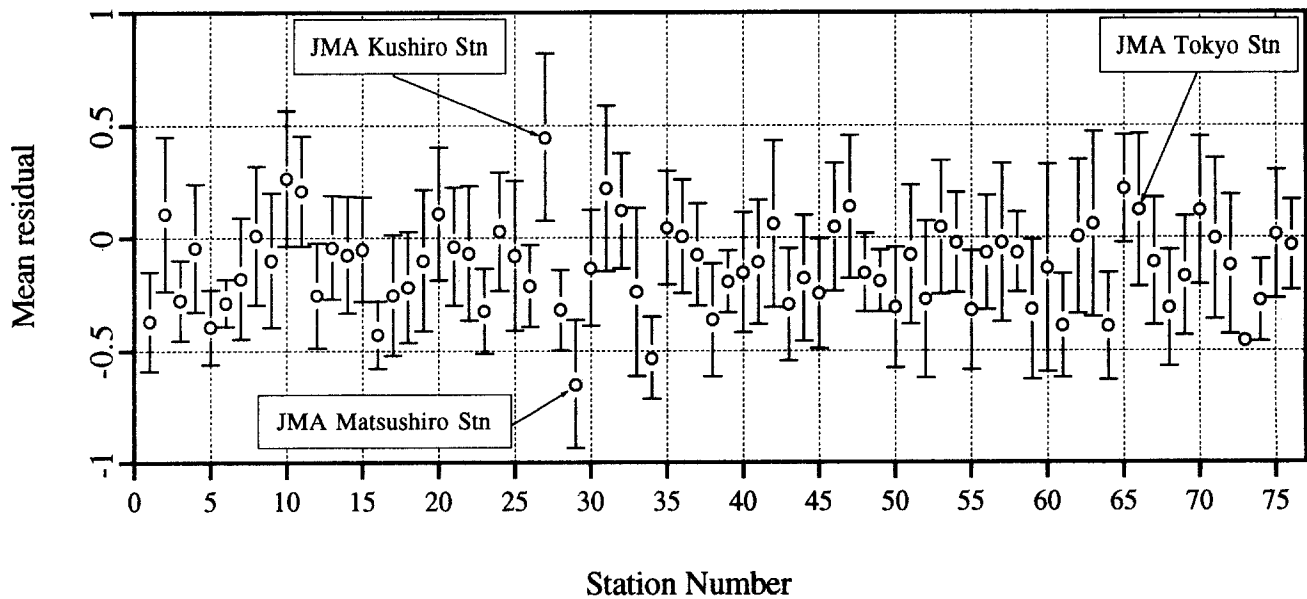
Figure 5.   Mean (open circles) and standard deviation (error bars) of the residuals from the regression of log PGA for each recording station in case 3 of Table 1. The JMA Kushiro station exhibits the largest amplification of the PGA. The JMA Matsushiro station, whose accelerometer is located in a rock tunnel, shows the smallest amplification.

results of the least-squares analysis if the effect of each recording station is considered. The R^2 statistic shows a significant increase; the standard deviation, σ, shows a marked decrease.

These preliminary analyses justify the inclusion of the depth term and the station coefficients in the attenuation model.

Method of Analysis

The regression model given in equation (2) is linear with respect to the coefficients to be determined. However, the correlation between magnitude and distance results in systematic errors if simple multilinear regression is used (Fukushima and Tanaka, 1990). They concluded that a two-stage regression method, introduced by Joyner and Boore (1981) to separate the distance dependence from the magnitude dependence, is desirable.

If the two-stage regression method were applied to equation (2), then the first stage is the least-squares regression of

$$\log y = \sum_{j=1}^{k} a_j A_j + b_2 r + b_3 \log r$$

$$+ b_4 h + \sum_{i=1}^{N-1} c_i S_i, \qquad (7)$$

where k is the number of earthquakes and $A_j = 1$ for earthquake j; $A_j = 0$ otherwise.

The second stage is the weighted least-squares regression of

$$a_j = b_0 + b_1 M_j, \qquad (8)$$

where a_j is determined in the first stage.

Equation (7) can be represented by

$$\mathbf{Y} = \mathbf{X}\boldsymbol{\beta} + \boldsymbol{\varepsilon}, \qquad (9)$$

where

$$\mathbf{X} = \begin{bmatrix} A_{1,1} & A_{2,1} & \cdots & A_{k,1} & r_1 & \log r_1 & h_1 & S_{1,1} & \cdots & S_{N-1,1} \\ A_{1,2} & A_{2,2} & \cdots & A_{k,2} & r_2 & \log r_2 & h_2 & S_{1,2} & \cdots & S_{N-1,2} \\ \vdots & \vdots & \vdots & \vdots & \vdots & \vdots & \vdots & \vdots & \vdots & \vdots \\ A_{1,n} & A_{2,n} & \cdots & A_{k,n} & r_n & \log r_n & h_n & S_{1,n} & \cdots & S_{N-1,n} \end{bmatrix}, \qquad (10)$$

and the solution is

$$\mathbf{b} = (\mathbf{X}^T\mathbf{X})^{-1} \mathbf{X}^T\mathbf{Y}. \qquad (11)$$

However, for this problem, $(\mathbf{X}^T\mathbf{X})$ is singular, most likely due to the large number of dummy variables involved. To solve equation (7), we propose the use of an iterative partial regression method to separate the determination of the two sets of dummy variables.

The two characteristics of this method are explained separately in the next sections.

Incremental Regression

Let the regression model be

$$y = b_0 + b_1 x_1 + b_2 x_2 + \ldots + b_p x_p + \varepsilon, \quad (12)$$

where y is the dependent variable, x_is are the independent variables, b_is are the regression coefficients to be determined, and ε is the residual. Equation (12) can be expressed in matrix form as

$$\begin{bmatrix} y_1 \\ y_2 \\ \vdots \\ y_n \end{bmatrix} = \begin{bmatrix} 1 & x_{11} & x_{21} & \ldots & x_{p1} \\ 1 & x_{12} & x_{22} & \ldots & x_{p2} \\ \vdots & \vdots & \vdots & \vdots & \vdots \\ 1 & x_{1n} & x_{2n} & \ldots & x_{pn} \end{bmatrix} \begin{bmatrix} b_0 \\ b_1 \\ \vdots \\ b_n \end{bmatrix} \begin{bmatrix} \varepsilon_1 \\ \varepsilon_2 \\ \vdots \\ \varepsilon_n \end{bmatrix}, \quad (13)$$

or in notation form as

$$\mathbf{Y} = \mathbf{X}\boldsymbol{\beta} + \boldsymbol{\varepsilon}, \quad (14)$$

and the least-squares solution is

$$\mathbf{b} = (\mathbf{X}^T\mathbf{X})^{-1}\mathbf{X}^T\mathbf{Y}. \quad (15)$$

Suppose that an initial estimate vector is given by $\mathbf{b}^*$, where

$$\mathbf{b}^* = [b_0^* \, b_1^* \, b_2^* \ldots b_p^*]^T. \quad (16)$$

We want to find an increment vector, $\Delta\mathbf{b}$, such that $\mathbf{b} = \mathbf{b}^* + \Delta\mathbf{b}$, where $\mathbf{b}$ is the least-squares solution. Equation (12) can be redefined as

$$y = (b_0^* + \Delta b_0) + (b_1^* + \Delta b_1) x_1 + (b_2^* + \Delta b_2) x_2 + \ldots + (b_p^* + \Delta b_p) x_p + \varepsilon. \quad (17)$$

Collecting terms and using the notation form,

$$\mathbf{Y} = \mathbf{X}\mathbf{b}^* + \mathbf{X}\Delta\boldsymbol{\beta} + \boldsymbol{\varepsilon}. \quad (18)$$

Let $\mathbf{Y}^* = \mathbf{X}\mathbf{b}^*$, then

$$\Delta\mathbf{Y} = \mathbf{Y} - \mathbf{Y}^* = \mathbf{X}\Delta\boldsymbol{\beta} + \boldsymbol{\varepsilon}, \quad (19)$$

and the solution is

$$\Delta\mathbf{b} = (\mathbf{X}^T\mathbf{X})^{-1}\mathbf{X}^T\Delta\mathbf{Y}. \quad (20)$$

By expanding the right-hand side of equation (20),

$$\Delta\mathbf{b} = [(\mathbf{X}^T\mathbf{X})^{-1}\mathbf{X}^T]\mathbf{Y} - [(\mathbf{X}^T\mathbf{X})^{-1}\mathbf{X}^T]\mathbf{Y}^*. \quad (21)$$

The first term of the right-hand side of equation (21) is the least-squares solution, $\mathbf{b}$, while the second term must be equal to the initial estimate vector, $\mathbf{b}^*$, from the definition

of $\mathbf{Y}^*$. Therefore, $\Delta\mathbf{b}$ satisfies the stated requirement that $\mathbf{b} = \mathbf{b}^* + \Delta\mathbf{b}$.

In summary, the least-squares solution can be determined in one step by adding the increment solution (equation 20) to the estimate vector. If the estimate vector is the null vector, then the incremental regression reverts back to the least-squares regression.

Partial Regression

Suppose that instead of determining all the increment coefficients of $\Delta\mathbf{b}$, we determine only a portion of the coefficients (say, Δb_0 and Δb_1). Then,

$$\text{let } y^* = b_0^* + b_1^* x_1 + b_2^* x_2 + \ldots + b_p^* x_p, \quad (22)$$

and

$$\Delta y = y - y^* = (\Delta b_0 + \Delta b_1 x_1) + (\Delta b_2 x_2 + \ldots + \Delta b_p x_p) + \varepsilon. \quad (23)$$

Thus, if

$$\Delta\mathbf{Y} = \mathbf{X}^i \begin{bmatrix} \Delta b_0 \\ \Delta b_1 \end{bmatrix} + \mathbf{X}^o \begin{bmatrix} \Delta b_2 \\ \vdots \\ \Delta b \end{bmatrix} + \varepsilon, \quad (24)$$

or

$$\Delta\mathbf{Y} = \mathbf{X}^i\Delta\boldsymbol{\beta}^i + (\mathbf{X}^o\Delta\boldsymbol{\beta}^o + \varepsilon), \quad (25)$$

then the solution is

$$\Delta\mathbf{b}^i = (\mathbf{X}^{iT}\mathbf{X}^i)^{-1}\mathbf{X}^{iT}\Delta\mathbf{Y}. \quad (26)$$

However, the expected value of $\Delta\mathbf{b}^i$ is

$$\begin{aligned} E(\Delta\mathbf{b}^i) &= (\mathbf{X}^{iT}\mathbf{X}^i)^{-1}\mathbf{X}^{iT} E(\Delta\mathbf{Y}) \\ &= (\mathbf{X}^{iT}\mathbf{X}^i)^{-1}\mathbf{X}^{iT}(\mathbf{X}^i\Delta\boldsymbol{\beta}^i + \mathbf{X}^o\Delta\boldsymbol{\beta}^o) \quad (27) \\ &= \Delta\boldsymbol{\beta}^i + (\mathbf{X}^{iT}\mathbf{X}^i)^{-1}\mathbf{X}^{iT}\mathbf{X}^o\Delta\boldsymbol{\beta}^o. \end{aligned}$$

Therefore, $\Delta\mathbf{b}^i$ is biased, and the amount of bias is given by the second term of the right-hand side of the equation. However, as $\Delta\boldsymbol{\beta}^o$ approaches 0, $E(\Delta\mathbf{b}^i)$ approaches $\Delta\boldsymbol{\beta}^i$. This can be achieved by iteratively incrementing $\mathbf{b}^{*i}$ with $\Delta\mathbf{b}^i$ and then changing the definition of $\mathbf{b}^{*i}$ to the other coefficients and then repeating the procedure until all increment vectors approach zero.

Implementation

The iterative partial regression method is used in this study as follows.

The first step determines the coefficients of the regression model given by equation 3 by one-stage multilinear regression. The coefficients thus solved serve as initial estimates.

Table 2
Data Grouping by Focal Depth

Data Group	Focal Depth Range (km)	Number of Events	Number of Records	Number of Stations
Group A	0.1–30	111	553	72
Group B	30–60	136	778	69
Group C	60–90	94	526	61
Group D	90–120	31	229	42
Group E	120–200	19	112	40
All	0.1–200	387	2166	76

The second and third steps are similar to the two-stage regression procedure of Joyner and Boore (1981). The second step is the multilinear regression of the equation

$$\log y = \sum_{j=1}^{K} a_j A_j + b_2 r + b_3 \log r + \underline{b_4} h + \sum_{i=1}^{N} \underline{c_i S_i}, \quad (28)$$

where $A_j = 1$ for the jth event (0 otherwise) and the underlined variables (b_4 and c_is) are constrained to the values determined in the previous step. The distance dependence of the attenuation is then determined. The third step is the regression of the equation

$$a_j = b_0 + b_1 M_j, \quad (29)$$

where a_j is determined in the previous step. The third step is carried out with a weighted least-squares procedure using the weighting matrix proposed by Joyner and Boore (1993). This step determines the magnitude dependence of the attenuation.

The first step is then repeated, except that b_1 to b_3 are constrained to the values from steps 2 and 3. The cycle is repeated until the coefficients stabilize. In this study, 10 iterations are sufficient to determine the regression coefficients.

Results and Discussion

Effect of Depth

To study the effect of depth on the attenuation characteristics of earthquake ground motions, we separated the data set into depth ranges (Table 2) with an interval of about 30 km, except for depths greater than 120 km, where the interval is bigger.

Resulting coefficients from iterative partial regression made on these data groups are given in Table 3 for PGA and in Table 4 for PGV. From Table 3, the anelastic attenuation term, b_2, decreases from group B to group E. This may be

Table 3
Regression Coefficients for Peak Ground Acceleration (PGA in cm/sec^2)

Group	b_0	b_1	b_2	b_3	b_4	c_i^*	σ_r	σ_e	σ
A	0.133	0.479	−0.00159	−1.00	0.00852	0.203	0.228	0.132	0.264
B	0.182	0.477	−0.00217	−1.00	0.00629	0.117	0.228	0.124	0.260
C	−0.430	0.575	−0.00176	−1.00	0.00643	0.211	0.221	0.101	0.244
D	−0.034	0.608	−0.00125	−1.00	−0.00197	0.548	0.201	0.055	0.209
E	−0.500	0.564	−0.00042	−1.00	0.00240	0.514	0.178	0.058	0.187
All	0.206	0.477	−0.00144	−1.00	0.00311	0.225	0.247	0.122	0.276

*For JMA Tokyo station.
σ_r^2 = record-to-record component of variance (determined in second step).
σ_e^2 = earthquake-to-earthquake component of variance (determined in third step).
σ^2 = total variance $\cong \sigma_r^2 + \sigma_e^2$.

Table 4
Regression Coefficients for Peak Ground Velocity (PGV in cm/sec)

Group	b_0	b_1	b_2	b_3	b_4	c_i^*	σ_r	σ_e	σ
A	−1.898	0.635	−0.00104	−1.00	0.00668	0.129	0.208	0.112	0.236
B	−1.847	0.630	−0.00197	−1.00	0.00594	0.100	0.224	0.109	0.250
C	−2.008	0.672	−0.00156	−1.00	0.00356	0.212	0.220	0.066	0.229
D	−1.701	0.710	−0.00124	−1.00	−0.00274	0.420	0.191	0.028	0.193
E	−2.498	0.702	−0.00070	−1.00	0.00333	0.348	0.180	0.072	0.194
All	−1.769	0.628	−0.00130	−1.00	0.00222	0.184	0.235	0.103	0.257

*For JMA Tokyo station.
σ_r^2 = record-to-record component of variance (determined in second step).
σ_e^2 = earthquake-to-earthquake component of variance (determined in third step).
σ^2 = total variance $\cong \sigma_r^2 + \sigma_e^2$.
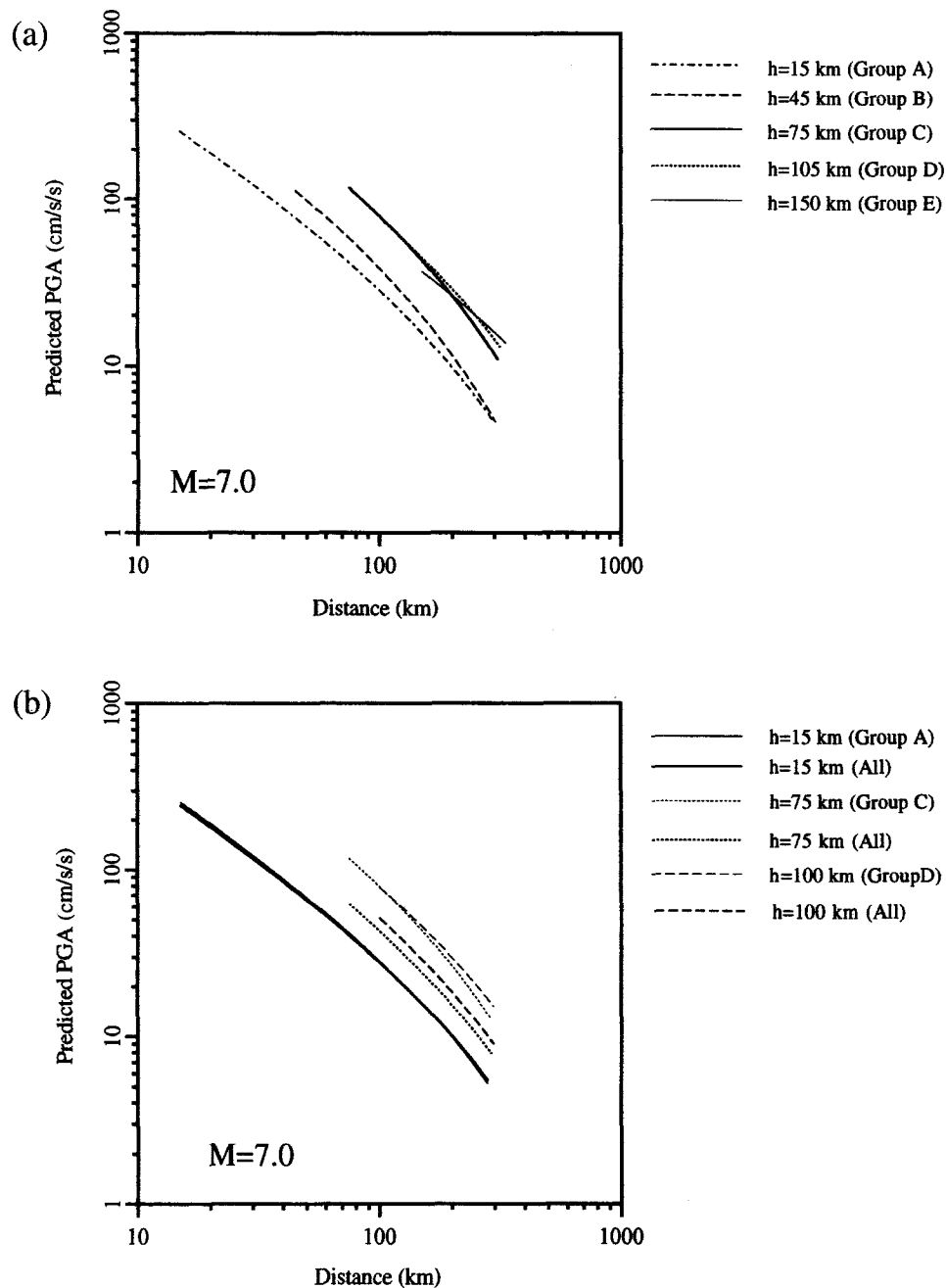
Figure 6.   Attenuation of PGA of magnitude 7.0 earthquake based on (a) regression of data grouped by depth (data grouping is defined in Table 2) and (b) comparison of attenuation curves from regression of whole data set and for selected data groups.

caused by the relatively higher-Q values in the deeper materials of the Earth's crust. We can also see a relatively larger depth term, b_4, for the groups with depths less than 90 km, while for those with depths greater than 90 km, the depth term becomes relatively small. This may be caused by the increasing range of depth, h, from group A to group E. If the depth effect, $b_4 h$, is compared, no systematic trend is observed. Group D has an irregular negative b_4 coefficient. This is consistent with the residual plot in Figure 4 where a slight negative correlation for the residual can be seen for

the depth range from 90 to 120 km. This may be caused by insufficient data for the deeper events, but this is still not conclusive until more data are acquired.

The physical significance of the depth term $b_4 h$ is still not clear. In this study, it is based primarily on statistical considerations (i.e., the behavior of the residuals), as in Crouse *et al.* (1988) and Annaka and Nozawa (1988). Deep events propagate in high-Q zones resulting in lower attenuation rates. In such case, the larger levels of peak amplitude can be explained by the lower attenuation rate, and the depth

Table 5

Classification of Ground Conditions for JMA Stations

Soil Condition	Geological Definition	Definition by Natural Period
Type 1 (rock)	tertiary or older rock (defined as bedrock), of diluvium with $H < 10$ m	$T < 0.2$ sec
Type 2 (hard soil)	diluvium with $H \geq 10$ m or alluvium with $H < 10$ m	0.2 sec $\leq T < 0.4$ sec
Type 3 (medium soil)	alluvium with $H < 25$ m including soft layer with thickness less than 5 m	0.4 sec $\leq T < 0.6$ sec
Type 4 (soft soil)	other than above, usually soft alluvium or reclaimed land	$T \geq 0.6$ sec

Figure 7. Attenuation of recorded PGA and PGA adjusted for station effect for the 1993 Kushiro-Oki earthquake. Solid line is the predicted PGA from the attenuation equation proposed in this study (using all data) with a station coefficient, $c_i = 0.0$.

term can be regarded as a correction factor to the attenuation rate. However, the depth effect is also evident for shallow events (e.g., for groups A and B) and this may be caused by factors other than the Q value. For example, this may be caused by the scattering of the seismic waves as it nears the surface resulting in an effective increase in the attenuation rate.

Figure 6a shows the plot of predicted PGA with respect to distance for magnitude 7.0 earthquakes with depths near the midpoint of the range in selected groups. The shapes of the attenuation curves for the data groups are similar, except for group E where the attenuation rate with respect to distance is lower. Except for group E, predicted PGA increases as the depth increases. In Figure 6a, the attenuation curves are plotted with $c_i = 0.0$, which represents the mean of the station coefficients in the data group. Since the data groups have a different number of stations, the relative position of the curves might be affected. Figure 6b compares the attenuation of the predicted PGA with respect to distance with the attenuation curves from stratified data for magnitude 7.0 earthquakes with different depths. The predicted PGAs from using all data are similar to those from stratified data for group A. For groups C and D, the difference becomes large although the attenuation rate is similar. It must be noted that these curves represent the mean of the station coefficients determined in the regression. Since the curves in Figure 6b consider the different number of stations, this may have an effect on the attenuation curves. The attenuation patterns for PGV are similar to those of PGA.

The number of records in each data group must be considered when comparing the regression results in Tables 3 and 4. Including station coefficients in the regression assumes that there are enough records for each recording station to establish the mean and standard deviation of the station coefficient. It must be realized that if there is only one record for one recording station, then the residual for that record will be zero. This may lead to bias in the least-squares analysis. For groups D and E, the data are few, and the num-

ber of records per station may not be enough. Thus, the results for these groups in Tables 3 and 4 may not be reliable. Fukushima and Tanaka (1990) corrected the observed data for each station by the average value of residuals between observed and predicted peak horizontal accelerations at the station. They reported that the standard deviation was reduced from 0.30 to 0.21 and that the multiple correlation coefficient increased from 0.81 to 0.89. However, a lot of their recording stations have only one record. Since the residuals are zero for these data, this may explain the very good fit they obtained.
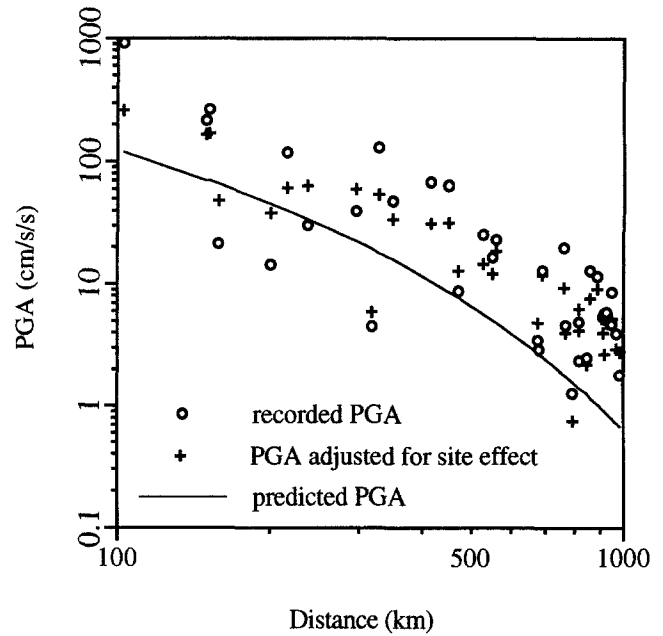
All things considered, the authors recommend the attenuation equations from the regression of all data for the PGA and PGV. This data set has a large number of records, making the determination of the station coefficients more reliable. This equation can also be used for shallow- to intermediate-depth earthquakes. These attenuation equations are used for the rest of this article. However, it must be noted that a proper station coefficient should be estimated before applying these equations. A station coefficient, $c_i = 0.0$, represents the mean of all station coefficients determined. However, this "mean" station will predict PGAs and PGVs lower than the PGAs and PGVs if station coefficients have not been considered. This may be explained by looking at Figure 5. In this figure, the mean residual for all records is zero; however, the mean residuals for many of the stations are below zero. This means that there is generally more records in stations with coefficients greater than zero than in stations with coefficients less than zero. This may be explained by the fact
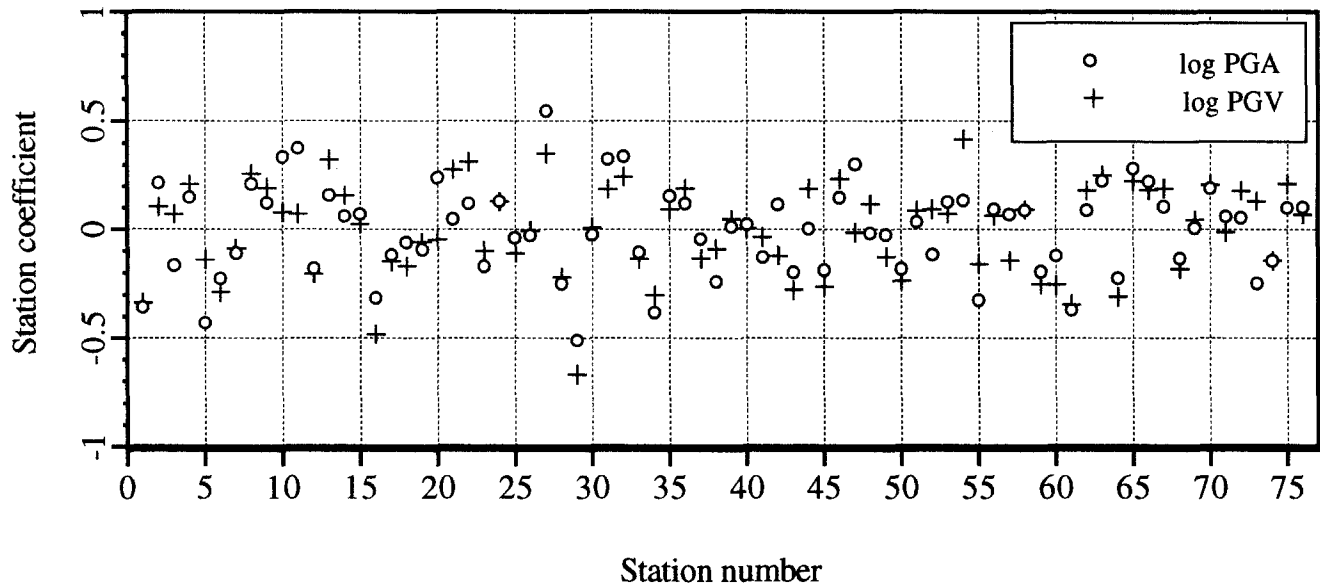
Figure 8. Station coefficients for log PGA and log PGV for JMA stations used in this study. The coefficients shown are determined using all data (see Tables 3 and 4). The mean of the station coefficients is zero for both the log PGA and log PGV. The weighted mean (with the number of records for each station used as weights) is 0.119 and 0.069 for the log PGA and log PGV, respectively.

that for the same base rock motion, high-amplification sites may detect motion at the surface, while low-amplification sites may not detect any significant motion. The weighted mean of the station coefficients (using the number of records per station as weights) is 0.1186 and 0.0687 for log PGA and log PGV, respectively.

Local Site Effect

Due to the large number of records for each station, it is possible to determine the station coefficient, which is a kind of correction term for the amplification/deamplification of the ground motions relative to other recording stations. It is generally accepted that softer soils tend to amplify the earthquake ground motion relative to rock and stiff soils. However, other local site conditions such as geology and topography may also affect amplification. By considering each recording station individually, these effects are automatically included.

The JMA recording stations are classified into four soil types according to the presence of soft layers. This classification is commonly used in Japan and is defined in Table 5. Preliminary analysis showed that the soil type is not statistically significant to show trends in the peak ground motion. The local site effect is demonstrated in Figure 7, which shows the recorded PGA, the adjusted PGA for site effect (by dividing the PGA with 10^{c_i}), and the predicted PGA (zero station coefficient) based on this study, for the 1993 Kushiro-Oki earthquake. It can be seen that variability of the PGA is reduced if the local site effect is considered and that most of the adjustments are in the direction of reduction of residuals. The JMA Kushiro station recorded a PGA of 917

cm/sec^2, but the adjusted PGA is only 260 cm/sec^2, which is much closer to the best fit line. The large amplification for the PGA of this station agrees with the study of Kawase (1994). The list of JMA stations and the resulting station coefficients are given in the Appendix and in Figure 8.

The distribution of the station coefficients with respect to the soil type is shown in Figure 9. In this figure, stations with unconfirmed soil types are not plotted. The mean station coefficient for each soil type is given by the horizontal line. A weak correlation for the PGA can be seen. For PGV, however, a stronger correlation exists in which the station coefficients increase as the ground becomes softer. However, the scatter of the station coefficients with respect to the soil type is still wide. If soil types are used to classify the data, the mean effect of all records in a given soil type will be used in the prediction. However, the results of this study show that this mean effect is significantly different from the mean effect of a single recording site. A common application of attenuation equations is for the seismic hazard estimation of a site. In this case, the situation is similar to that of a single recording site. Therefore, if the proper site coefficient is obtained, the determination of the seismic hazard will be more accurate, and the variability will be reduced.

Comparison

Figure 10 shows the attenuation of the predicted PGA developed in this study (for all data) and other attenuation relations for Japan for magnitudes 5.0 and 7.0 earthquakes. The station coefficient, c_i, is set to the weighted mean of the station coefficients (i.e., $c_i = 0.119$ for PGA; $c_i = 0.069$ for PGV). Since the definitions of distance and response variable
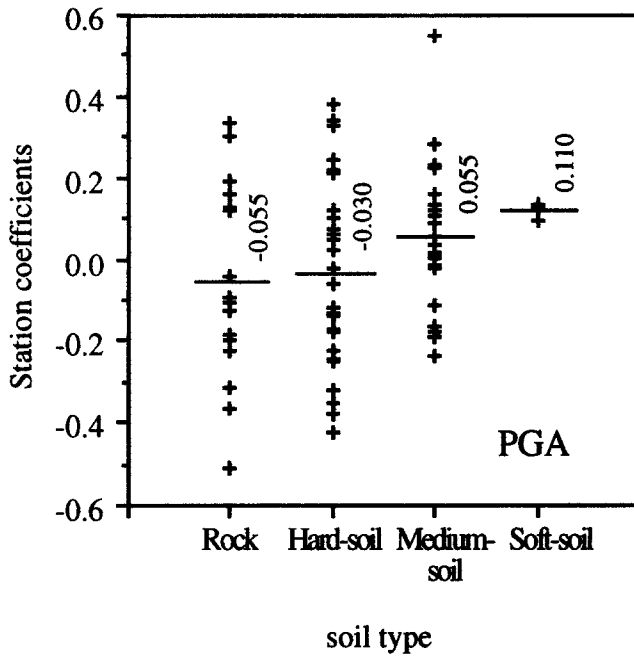
(a)
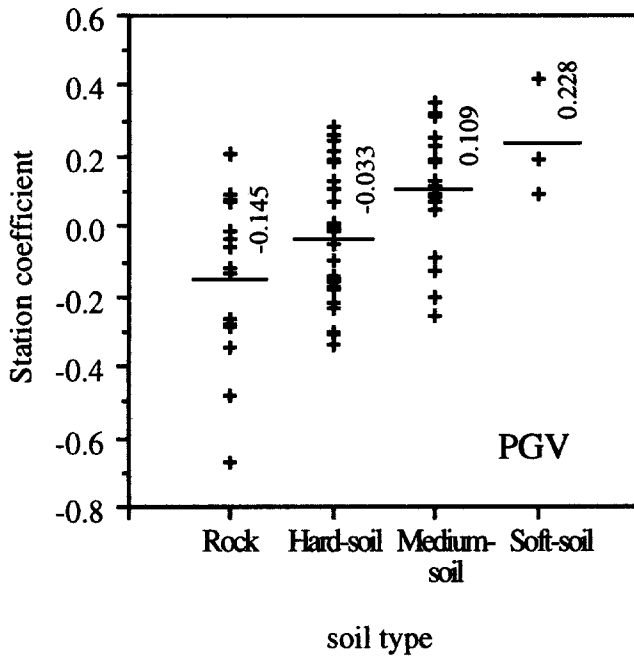
(b)

Figure 9. Plot of station coefficients for the (a) PGA and (b) PGV with respect to the soil type classification of JMA stations. Horizontal bars and numbers show the mean coefficient per soil type. The coefficients shown are determined using all data (see Tables 3 and 4).

are sometimes different, some assumptions are used. The comparison of the databases used in the attenuation studies is given in Table 6.

Kawashima *et al.* (1986) proposed the equations

$$\log PGA = 2.3664 \\ + 0.313M - 1.218 \log(\Delta + 30), \text{ and} \quad (30a)$$

$$\log PGV = 0.4487 \\ + 0.430M - 1.222 \log(\Delta + 30), \quad (30b)$$

where PGA (cm/sec^2) and PGV (cm/sec) are the maximum resultants from the combination of the two horizontal components in the time domain, M is the magnitude, and Δ is the epicentral distance, for the attenuation of PGA in soil (soil type 2). It must be noted, however, that soil type 2 used by Kawashima *et al.* is the combined soil types 2 and 3 used in this study. This equation does not consider the depth of the source. The analysis was made from Japanese earthquakes with focal depths up to 60 km. In Figure 10, the plotted distance is assumed to be $\sqrt{(\Delta^2 + h^2)}$.

Annaka and Nozawa (1988) used the attenuation equations

$$\log PGA = 0.627M \\ + 0.00671H - 2.212 \log D + 1.711, \text{ and} \quad (31a)$$

$$\log PGV = 0.795M \\ + 0.00550H - 2.065 \log D + 0.212, \quad (31b)$$

where PGA (cm/sec^2) and PGV (cm/sec) are the means of the peak acceleration from two horizontal components at each site, M is the magnitude, H is the depth of the point on the fault plane in kilometers when r becomes the closest distance in kilometers to the fault plane, and D is the distance parameter, defined as

$$D = r + 0.35 \exp(0.65M). \quad (32)$$

In Figure 10, r is assumed to be equal to the distance used in this study, and H is assumed to be equal to the depth. The attenuation equations are for ground with a shear wave velocity, $V_s \geq 300$ m/sec. If the ground motion is recorded in the surface ground with V_s less than 300 m/sec, it is converted by one-dimensional wave propagation theory into incident motions at the base layer, where $V_s \geq 300$ m/sec.

Fukushima and Tanaka (1990) proposed the equation

$$\log PGA = 0.41M - \log(r + 0.032 \cdot 10^{0.41M}) \quad (33) \\ - 0.0034r + 1.30,$$

where PGA (cm/sec^2) is the mean of the peak acceleration from two horizontal components at each site, r is the shortest distance between the site and fault rupture (kilometers), and M is the surface-wave magnitude. The data set used in their analysis comprises Japanese earthquakes with focal depths
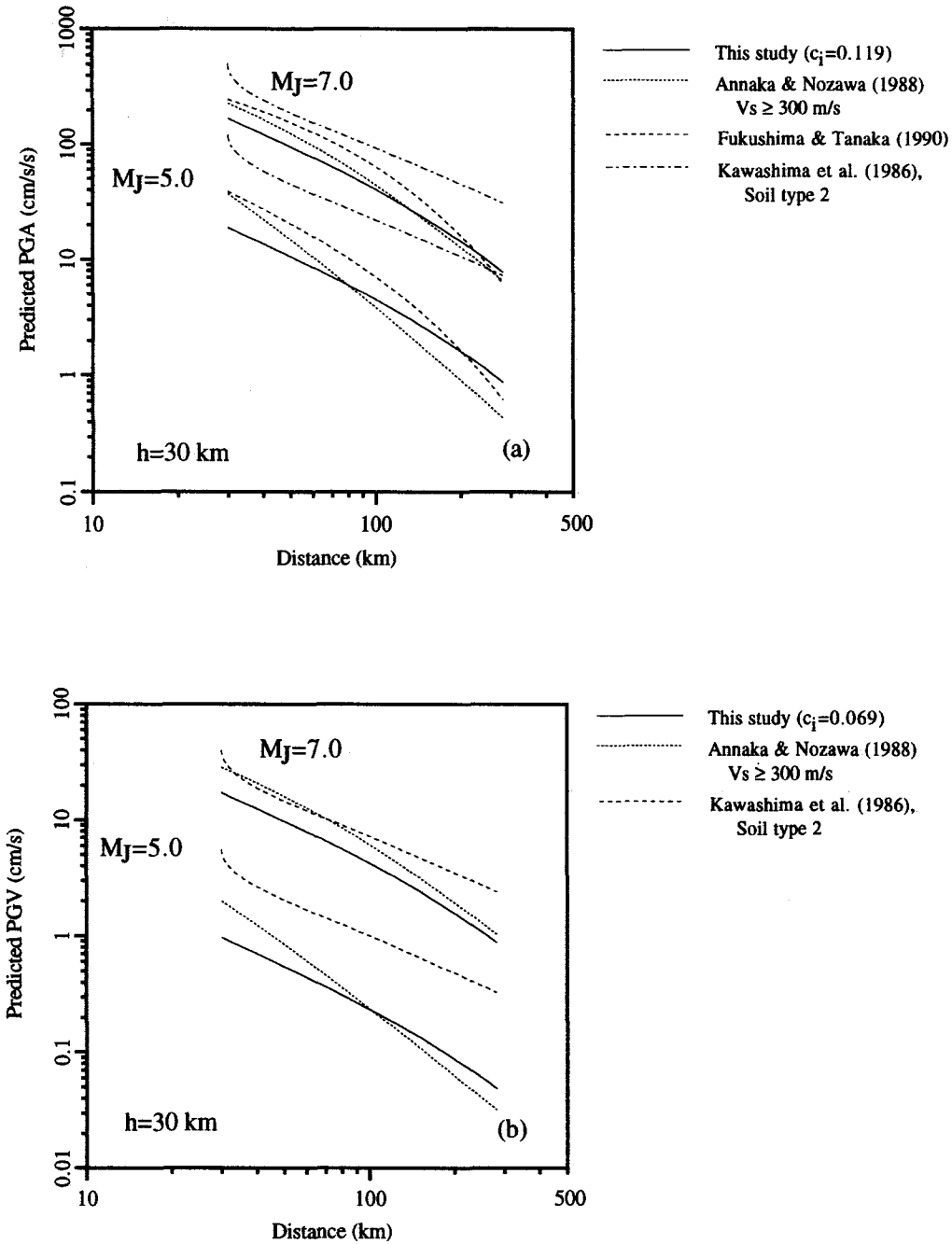
Figure 10. Comparison of attenuation equations for (a) PGA and (b) PGV of this study and previous results for JMA magnitude 5.0 and 7.0 earthquakes with depth of 30 km. In the case of Annaka and Nozawa (1988), observed motions recorded in the ground surface where the shear-wave velocity, V_s, is less than 300 m/sec were converted into incident motions at the base layer, where V_s is greater than 300 m/sec. Soil type 2 of Kawashima *et al.* (1986) is a combination of soil types 2 and 3 given in Table 5.

up to 30 km and is supplemented by U.S. records taken in the near source. In Figure 10, the JMA magnitude is converted to the surface-wave magnitude by (Hayashi and Abe, 1984) the following:

$$M_S = 1.27M_J - 1.82. \qquad (34)$$

Since the definitions of the PGA are different, the PGAs

are adjusted in accordance with the mean ratios of the different definitions (Ansary *et al.*, 1994). Ansary *et al.* analyzed a subset of the data used in this study. For PGA, the mean ratio (L/R) of the larger of the two horizontal components (used in this study) with respect to the resultant (used by Kawashima *et al.*, 1986) is given as 0.934 while the mean ratio (L/A) of the larger of the two horizontal components with respect to the mean of the two (used by Annaka

Table 6
Comparison of Databases of Attenuation Studies in Japan

Study	Kawashima *et al.* (1986)	Annaka and Nozawa (1988)	Fukushima and Tanaka (1990)	This Study
Number of records (two component pairs)	197	319	200 (USA), 486 (Japan)	2166
Number of earthquakes	90	45	15 (USA), 28 (Japan)	387
Minimum magnitude	$M_{JMA} \geq 5.0$	$M_{JMA} \geq 3.9$	$M_{JMA} \geq 5.0$ (Japanese data)	$M_{JMA} \geq 4.0$
Depth	$h \leq 60$ km	$h \leq 100$ km	$h \leq 20$ km (USA), $h \leq 30$ km (Japan)	$h \leq 200$ km, $h \neq 0$ km
Minimum acceleration	not specified	not specified (0.3 cm/sec^2)	predicted PGA ≥ 10 cm/sec^2	PGA ≥ 1 cm/sec^2 for both horizontal components
Recording stations Other criteria	67 (free-field)	41 (free-field)	not specified more than three records per earthquake	76 (free-field)
Definition of maximum	maximum resultant of combination of two horizontal components	mean of two horizontal components	mean of two horizontal components	larger of two horizontal components
Instrument	corrected SMAC	Sabo-type accelerometers with flat sensitivity between 0.2 and 30 Hz	various, including uncorrected SMAC	JMA 87-type–accelerometers

and Nozawa, 1988; and Fukushima and Tanaka, 1990) is given as 1.11. For PGV, the L/R ratio is 0.926 while the L/A ratio is 1.13.

Figure 10a shows the predicted mean PGA of this study and of previous studies for events with JMA magnitudes of 5.0 and 7.0 and a depth of 30 km. The attenuation rate with respect to distance is smaller than those of Annaka and Nozawa (1988) and Fukushima and Tanaka (1990) but larger than that of Kawashima *et al.* (1986). The smaller attenuation rates determined in this study may be caused by the use of data in the high-Q zone for deep events and from the exclusion of data lower than 1 cm/sec^2. The equation of Kawashima *et al.* (1986) does not consider the depth, resulting in higher predicted ground motion, especially at small distances. The same trend can be seen for PGV (Fig. 10b). The attenuation curves for specific stations will be higher or lower than the reference curve, depending on the value of the station coefficient.

Conclusions

Results of a regression study of ground motion recorded by the new JMA-87–type accelerometers from 76 Japan Meteorological Agency recording stations are reported. The use of these new records is significant because there is no need to correct for suppressed instrument sensitivity in the high-frequency range. Having considered earthquakes with depths of up to 200 km, the attenuation equations thus obtained can be used for subduction zone earthquakes.

Since there are many records for most of the stations, the effect of the local site on the variation of the peak ground motion is considered. Preliminary regressions on the data set

show a significant effect of the depth and the local site on the multilinear regression.

Due to the correlation between the magnitude and distance, a two-stage procedure is used to separate the determination of the distance dependence from the magnitude dependence. However, in considering the local site effect of each recording station, additional dummy variables are used in the regression, and the solution of the normal equations becomes singular. An iterative partial regression procedure is proposed to estimate the coefficients of the independent variables.

The peak ground motion was found to increase as the depth of the source increases. This effect is significant for depths up to 100 km.

Station coefficients are used to determine the effects of each recording station and were found to be weakly correlated with the soil classification in the case of PGA, while a stronger correlation was found for the PGV. In both cases, however, the variation is wide such that the use of soil classification alone cannot effectively describe the proper amplification/deamplification for each recording station. This is significant for seismic hazard estimation because the situation is similar to a single recording station. The use of station coefficients decreases the variability of the attenuation of the PGA and PGV.

Attenuation equations for the PGA and PGV that can be used for source depths of up to 200 km are proposed.

References

Abrahamson, N. A. and J. J. Litehiser (1989). Attenuation of vertical peak acceleration, *Bull. Seism. Soc. Am.* **79**, 549–580.

Annaka, T. and Y. Nozawa (1988). A probabilistic model for seismic hazard estimation in the Kanto district, *Proc. 9th World Conf. Earthquake Eng.* **2**, 107–112.

Ansary, M. A., F. Yamazaki, and T. Katayama (1994). Peak values of ground motion indices based on two horizontal components, *Proc. 9th Japan Earthquake Eng. Symp.* **3**, E37–E42.

Boore, D. M. and W. B. Joyner (1982). The empirical prediction of ground motion, *Bull. Seism. Soc. Am.* **72:6**, S43–S60.

Campbell, K. W. (1985). Strong ground motion attenuation relationships: A ten-year perspective, Earthquake Spectra **1:4**, 759–804.

Crouse, C. B., Y. K. Vyas, and B. A. Schell (1988). Ground motions from subduction-zone earthquakes, Bull. Seis. Soc. Am. **78**, no. 1, 1–25.

Draper, N. and H. Smith (1981). *Applied Regression Analysis*, Second Ed., Wiley, New York.

Fukushima, Y. and T. Tanaka (1990). A new attenuation relation for peak horizontal acceleration of strong earthquake ground motion in Japan, *Bull. Seism. Soc. Am.* **80**, no. 4, 757–783.

Hayashi, Y. and K. Abe (1984). A method of Ms determination from JMA data, *J. Seism. Soc. Japan* **37**, 429–439 (in Japanese).

Japan Meteorological Agency (JMA) (1991). Earthquake Observer Guide. (In Japanese)

Joyner, W. B. and D. M. Boore (1981). Peak horizontal acceleration and velocity from strong-motion records including records from the 1979 Imperial Valley, California, earthquake, *Bull. Seism. Soc. Am.* **71**, 2011–2038.

Joyner, W. B. and D. M. Boore (1988). Measurement, characterization and prediction of strong motion, in *Proc. of the ASCE Conf. on Earthquake Engineering Soil Dyn.*, Park City, Utah, 43–102.

Joyner, W. B. and D. M. Boore (1993). Methods for regression analysis of strong-motion data, *Bull. Seism. Soc. Am.* **83**, 469–487.

Kagami, H. (1993). Damage survey of the 1993 Kushiro-Oki earthquake, Report of Japan Ministry of Education, Science, and Culture, Grant No. 04306025, 19–25 (in Japanese).

Kawase, H. (1994). Strong motion characteristics observed at JMA stations in Hokkaido. *J. Struct. Constr. Eng.*, AIJ. No. 459, 57–64 (in Japanese).

Kawashima, K., K. Aizawa, and K. Takahashi (1986). Attenuation of peak ground acceleration, velocity and displacement based on multiple regression analysis of Japanese strong motion records, *Earthquake Eng. Struct. Dyn.* **14**, 199–215.

Kawashima, K., Y. Takagi, and K. Aizawa (1982). Accuracy of digitization of strong-motion records obtained by SMAC-accelerograph, *Proc. Japan Soc. Civil Engineers*, no. 323, 67–75.

McGuire, R. K. (1978). Seismic ground motion parameter relations, *J. Geotech. Eng. Div., ASCE* **104**, 481–490.

Nakanishi, I. and M. Kikuchi (1993). Characteristics of the 1993 Hokkaido-Nansei-Oki earthquake, *J. Japan Soc. Earthquake Eng. Promotion (NEWS)*, no. 133, 1–5 (in Japanese).

Ohno, S., T. Ohta, T. Ikeura, and M. Takemura (1993). Revision of attenuation formula considering the effect of fault size to evaluate strong motion spectra in near field, *Tectonophysics* **218**, 69–81.

Singh, S. K., M. Ordaz, J. G. Anderson, M. Rodriguez, R. Quass, E. Mena, M. Ottaviani, and D. Almora (1989). Analysis of near-source strong-motion recordings along the Mexican subduction zone, *Bull. Seism. Soc. Am.* **79**, 1697–1717.

Appendix
List of Japan Meteorological Agency Stations

Station Number	Station Code	Station Name	Latitude (N)	Longitude (E)	Soil Type	Number of records	Station Coefficient, c_i	
							(PGA)	(PGV)
1	ABJ	Abashiri	44.015	144.283	2	14	−0.3557	−0.3358
2	AJI	Ajiro	35.043	139.097	2	80	0.2172	0.1050
3	AKI	Akita	39.715	140.103	3	17	−0.1653	0.0703
4	AOM	Aomori	40.820	140.773	4(*)	56	0.1512	0.2101
5	ASA	Asahikawa	43.770	142.373	2	7	−0.4276	−0.1396
6	ASZ	Ashizuri	32.720	133.013	1	3	−0.2241	−0.2861
7	CHO	Choshi	35.737	140.862	2(*)	48	−0.1085	−0.0886
8	FKK	Fukuoka	33.580	130.380	2	6	0.2127	0.2586
9	FUK	Fukui	36.053	136.227	4	16	0.1244	0.1939
10	FUN	Kawaguchiko	35.498	138.763	1	36	0.3369	0.0786
11	HAC	Hachinohe	40.525	141.525	2	107	0.3788	0.0723
12	HAK	Hakodate	41.815	140.758	3	38	−0.1789	−0.2041
13	HIK	Hikone	35.273	136.247	3	15	0.1611	0.3232
14	HIR	Hiroshima	34.395	132.465	2(*)	12	0.0620	0.1572
15	HJJ	Hachijojima	33.102	139.788	2(*)	40	0.0721	0.0249
16	HMD	Hamada	34.893	132.073	1	5	−0.3126	−0.4815
17	HMM	Hamamatsu	34.707	137.723	2	16	−0.1176	−0.1479
18	IID	Iida	35.510	137.837	2	20	−0.0588	−0.1702
19	ISI	Ishigakijima	24.332	124.163	1	8	−0.0915	−0.0605
20	ISN	Ishinomaki	38.425	141.303	2	48	0.2420	−0.0479
21	KAG	Kagoshima	31.573	130.553	2	9	0.0492	0.2786
22	KAN	Kanazawa	36.587	136.637	3	10	0.1225	0.3122
23	KOB	Kobe	34.688	135.180	2	4	−0.1692	−0.0998
24	KOF	Kofu	35.665	138.557	3	48	0.1324	0.1286
25	KTR	Katsuura	35.148	140.315	3(*)	28	−0.0379	−0.1084
26	KUM	Kumamoto	32.810	130.710	2	7	−0.0254	−0.0071
27	KUS	Kushiro	42.975	144.392	3	56	0.5473	0.3516
28	MAE	Maebashi	36.402	139.065	2	31	−0.2486	−0.2204
29	MAT	Matsushiro	36.547	138.213	1	2	−0.5085	−0.6683

Appendix
Continued

Station Number	Station Code	Station Name	Latitude (N)	Longitude (E)	Soil Type	Number of records	Station Coefficient, c_i (PGA)	Station Coefficient, c_i (PGV)
30	MIS	Mishima	35.112	138.930	2	39	−0.0232	0.0073
31	MIT	Mito	36.378	140.472	2	100	0.3285	0.1874
32	MRK	Morioka	39.697	141.167	2	103	0.3394	0.2450
33	MRT	Murotomisaki	33.248	134.180	1	4	−0.1056	−0.1369
34	MTM	Matsumoto	36.243	137.973	2	10	−0.3798	−0.3018
35	MTS	Matsue	35.455	133.072	1	7	0.1569	0.0925
36	MTY	Matsuyama	33.840	132.780	2	7	0.1224	0.1909
37	MYK	Miyakojima	24.792	125.278	1	3	−0.0422	−0.1338
38	MYZ	Miyazaki	31.920	131.423	3	13	−0.2380	−0.0906
39	MZH	Maizuru	35.448	135.320	3(*)	6	0.0156	0.0471
40	NAG	Nagoya	35.165	136.968	2	19	0.0242	0.0055
41	NAH	Naha	26.203	127.690	1	6	−0.1257	−0.0357
42	NEM	Nemuro	43.328	145.590	1	40	0.1169	−0.1207
43	NGT	Irozaki	34.600	138.847	1	23	−0.1962	−0.2774
44	NII	Niigata	37.910	139.052	3	12	0.0053	0.1895
45	NOB	Nobeoka	32.578	131.660	1	5	−0.1865	−0.2613
46	NZJ	Naze	28.377	129.498	3(*)	12	0.1497	0.2349
47	OFU	Ofunato	39.062	141.718	1	79	0.3042	−0.0143
48	OIT	Oita	33.233	131.623	3	10	−0.0162	0.1177
49	OKA	Okayama	34.658	133.918	2	13	−0.0230	−0.1266
50	OMA	Omaezaki	34.603	138.213	2	16	−0.1800	−0.2351
51	ONA	Onahama	36.945	140.907	3	79	0.0369	0.0870
52	OSA	Osaka	34.678	135.522	3	5	−0.1143	0.0933
53	OSH	Oshima	34.747	139.367	1	58	0.1289	0.0726
54	SAK	Sakata	38.907	139.847	4	19	0.1360	0.4173
55	SAP	Sapporo	43.058	141.332	2	15	−0.3218	−0.1588
56	SEN	Sendai	38.260	140.900	2(*)	66	0.0962	0.0642
57	SHJ	Shionomisaki	33.448	135.763	2	4	0.0720	−0.1429
58	SHN	Shimonoseki	33.945	130.928	4	6	0.0911	0.0925
59	SHZ	Shizuoka	34.973	138.407	3	32	−0.1922	−0.2515
60	SUT	Suttsu	42.793	140.228	2(*)	7	−0.1190	−0.2537
61	TAJ	Tanegashima	30.737	130.993	1	6	−0.3678	−0.3432
62	TAT	Tateyama	34.983	139.868	3	65	0.0903	0.1813
63	TKD	Takada	37.105	138.250	3	13	0.2282	0.2523
64	TKY	Takayama	36.153	137.257	2	10	−0.2214	−0.3088
65	TMR	Tomakomai	42.623	141.585	3	56	0.2839	0.2256
66	TOK	Tokyo	35.687	139.758	3	99	0.2249	0.1843
67	TOT	Tottori	35.485	134.240	3	7	0.1091	0.1914
68	Toy	Toyama	36.707	137.205	2	13	−0.1307	−0.1805
69	TSU	Tsu	34.730	136.523	3	12	0.0108	0.0450
70	URA	Urakawa	42.158	142.782	1	84	0.1942	0.2088
71	UTS	Utsunomiya	36.547	139.872	2	65	0.0631	0.0123
72	WAJ	Wajima	37.390	136.898	3	17	0.0564	0.1805
73	WAK	Wakkanai	45.413	141.683	2	2	−0.2464	0.1330
74	WKM	Wakamatsu	37.485	139.913	2(*)	27	−0.1419	−0.1428
75	YOK	Yokohama	35.437	139.657	2	82	0.1028	0.2124
76	YON	Yonago	35.432	133.342	3	3	0.1046	0.0704

Notes:

(*) denotes unconfirmed soil type classification.

Station coefficients shown are determined from regression of all data.

JMA stations in Izuhara and Uwajima are not included because they do not have records used in this study.

Institute of Industrial Science
The University of Tokyo
7-22-1 Roppongi
Minato-Ku, Tokyo 106, Japan
   (G.L.M., F.Y.)